Evidence for the Structure of the Active Site Heme P460 in Hydroxylamine Oxidoreductase of *Nitrosomonas*†

David M. Arciero,‡ Alan B. Hooper,‡ Mengli Cai,§ and Russell Timkovich*,§

Department of Genetics and Cell Biology, University of Minnesota, St. Paul, Minnesota 55108, and Department of Chemistry, University of Alabama, Tuscaloosa, Alabama 35487-0336

Received May 7, 1993; Revised Manuscript Received June 29, 1993®

ABSTRACT: Hydroxylamine oxidoreductase (HAO) is responsible for the oxidation of hydroxylamine to nitrite in nitrification by *Nitrosomonas europaea*. It has an α_n subunit structure and eight covalently bound hemes per subunit. Seven of these have visible spectra indistinguishable from heme *c*. The eighth, designated as P460, has unusual visible spectroscopic features in the enzyme and in a heme-containing proteolytic fragment. Its structure has not been previously determined. Enzymatic digestions of HAO were performed, and various proteolytic fragments were purified. Mass spectrometry confirmed the presence of authentic heme *c* in some fragments, that is, iron protoporphyrin IX cross-linked by two thioether bonds to cysteine residues. It was possible to detect the presence of the P460 pigment in some fragments, based upon the sensitivity of this pigment to treatment of the holoenzyme with hydrogen peroxide. A proteolytic fragment produced by sequential digestion with trypsin and pronase was shown to contain heme *c* and a hydrogen peroxide-sensitive heme with an unusual visible spectrum. This fragment contained two covalently cross-linked peptides. Mass spectrometry and NMR indicated that the P460 heme was iron protoporphyrin IX covalently bonded by two thioether bridges to peptide, but in addition there was a new, third covalent bond between a meso heme carbon and an aromatic ring carbon on a tyrosyl residue. The new covalent bond has been tentatively assigned to the C2 carbon of the tyrosyl ring and the 5-*meso* heme carbon (IUPAC-IUB tetrapyrrole nomenclature), although this location requires further proof.

In the global nitrogen cycle, nitrifying bacteria aerobically convert ammonia to nitrite. In *Nitrosomonas europaea*, ammonia is converted to hydroxylamine, and then hydroxylamine is oxidized to nitrite by hydroxylamine oxidoreductase (HAO).[1] On the basis of recent sequencing studies (Arciero & Hooper, 1993), HAO is now known to be an oligomer ($\alpha 2$ or $\alpha 3$) of a 63-kDa subunit that contains eight covalently bound hemes. These multiple hemes can be differentiated on the basis of visible, EPR, Mossbauer, and resonance Raman spectra, as well as differences in redox properties and reduction kinetics (Hooper et al., 1978, 1984; Lipscomb & Hooper, 1982; Lipscomb et al., 1982; Prince et al. 1983; Prince & Hooper, 1987; Andersson et al., 1984, 1991). Visible spectroscopic data indicated that the major type of heme present was heme *c*. One heme, termed P460, was an enigma. The visible spectrum of HAO in the resting oxidized state looked like a typical low-spin ferricytochrome *c*. Upon reduction by dithionite, it appeared as a typical low-spin ferrocytochrome *c* except for the presence of a band at 463 nm. It has been difficult to study this pigment because of the high number (seven) of spectroscopically assigned *c*-type hemes. Thus the ferrous pyridine hemochromogen spectrum of HAO only showed the α, β, and Soret bands expected for heme *c*. The importance of the P460 center was recognized early, for it was the CO binding site in the reduced state. Hooper and Terry (1977) showed that when HAO was treated with hydrogen peroxide, there was a rapid and irreversible loss of the ability to oxidize hydroxylamine. Concomitant with this inactivation was the loss of the ferrous P460 spectral signature, while the bands attributable to *c* hemes were unchanged.

This paper presents evidence for the identity of the active site P460 heme in *Nitrosomonas* HAO.

MATERIALS AND METHODS

Proteolytic digestions of HAO were carried out as described previously (Arciero & Hooper, 1993), and nomenclature of peptides follows that established in the earlier work. Peptide T7 refers to a tryptic peptide derived from HAO, and peptide T7C, refers to a chymotryptic peptide derived from subdigestion of peptide T7. Peptides Pr1 and Pr2 refer to heme peptides derived from the pronase digestion of T7 or T7C. The procedure for isolation of peptides T7 and T7C followed procedures described previously (Arciero & Hooper, 1993). To summarize, after digestion of HAO with trypsin, heme peptides were precipitated quantitatively with ammonium sulfate (at 70% saturation) and then resolubilized in a minimal volume of 20 mM H_3PO_4. Heme peptides were then fractionated on a Spherogel TSK 2000SW HPLC gel filtration column equilibrated with 20 mM H_3PO_4. Peptide T7 was the first peak but was heterogeneous when analyzed by reverse-phase HPLC. Peptide T7 was digested with chymotrypsin in 0.1 M Tris/acetate buffer at pH 8.3 and then fractionated by reverse-phase HPLC using TFA/acetonitrile as described previously (Arciero & Hooper, 1993). Sequence analysis indicated that peptides T7 and T7C differed only in their C-terminal portions away from the heme binding sites and that T7 heterogeneity was mainly due to variable C-termini.

† Financial support was provided in part by NIH Grant GM43292 (R.T.) and NSF Grant DMB-9019687 (A.B.H.).

* To whom correspondence should be addressed.

‡ University of Minnesota.

§ University of Alabama.

® Abstract published in *Advance ACS Abstracts*, August 15, 1993.

[1] Abbreviations: HAO, hydroxylamine oxidoreductase; LSIMS, liquid secondary ion mass spectrometry; MS, mass spectrometry; PTH, phenylthiohydantoin; cyt, cytochrome.

0006-2960/93/0432-9370$04.00/0

To produce smaller heme peptides, peptide T7 or T7C was further digested with 0.5% (w/w) *Streptomyces griseus* pronase (Calbiochem) in 0.1 M Tris/acetate buffer, pH 7.6, at 37 °C. Typical digestion time was 6 h, but some digestions involved much longer times (as discussed in Results). Peptides were fractionated by reverse-phase HPLC as described above. In the larger scale digestions, up to four major fractions were obtained. One, designated Pr2, eluted at circa 19–20 m. Three others, designated Pr1a, Pr1b, and Pr1c, were clustered between 5 and 7 m. Pronase produced a heterogeneous mixture, and several minor fractions were observed between 7 and 19 m that were too dilute for further analysis.

Conditions for liquid secondary ion mass spectrometry (LSIMS, also known as fast atom bombardment, or FAB, mass spectrometry) have been described (Carraway et al., 1993). LSIMS spectra produce a cluster of peaks differing by 1 mass unit around the monoisotopic mass of the ion observed. These are due to hydrogen rearrangements and the statistical distribution of mainly ^{13}C. The observed m/z value of the tallest peak in the cluster will be reported. Normally, for LSIMS this corresponds to the $(M + H)^+$ ion, although other adducts are known, corresponding to the addition of sodium, potassium, or ammonium ions, even though these cations may only be present at trace contaminant levels in the matrix. Low-resolution spectra were obtained at $\Delta m/m$ 1000 (10% valley definition), and m/z values rounded to the nominal integer mass will be reported, except for high values, which will be reported to within 0.1 Da, because the mass excess of hydrogen can lead to confusion between nominal and observed mass. When the number of carbon atoms per molecule exceeds 45, the statistical probability of any one molecule containing at least one ^{13}C (natural abundance 1.1%) is greater than 50%; therefore, calculations of nominal mass should include at least one ^{13}C. For typical peptides this is around 1500 Da. High-resolution spectra were obtained at a resolution of 10 000, and polyethylene glycol was used as internal mass reference.

NMR spectra were obtained on a Bruker AM360 or AM500 spectrometer, in temperature-regulated 5-mm probes in 99.9% deuterium oxide, buffered with 50 mM deuterated ammonium bicarbonate to pD 8.3. Chemical shifts are reported versus sodium 3-(trimethylsilyl)tetradeuteropropionate, but the residual water peak was used as an indirect reference standard. Further spectroscopic details were similar to the conditions reported in Chau et al. (1990). Ferrous, CO-complexed samples were prepared by dissolving dried amounts of the peptides in deoxygenated buffer and further removing oxygen by cycles of vacuum and argon. Solid sodium dithionite was added under a blanket of argon, and then the sample was further purged by cycles of vacuum and carbon monoxide. Samples were finally sealed under 500 Torr of carbon monoxide. Heme peptides from horse heart cyt *c* were prepared as described by Carraway et al. (1993).

RESULTS

Identification of the P460 Heme Peptide in a Multi-Heme Protein. No hemes were liberated from HAO by standard extraction experiments. The P460 heme of native HAO is distinguishable from other hemes by its unusual band at 463 nm in the dithionite-reduced enzyme. However, this band was no longer observed in the denatured dithionite-reduced enzyme, thereby complicating its isolation. One of the heme-containing peptides released by trypsin digestion had an atypical absorption spectrum compared to other heme peptides. However, this did not provide structural information, because it was possible that an unusual ligand arrangement was responsible for the differences. It was essential to determine with certainty which heme peptide from HAO contained the P460 heme.

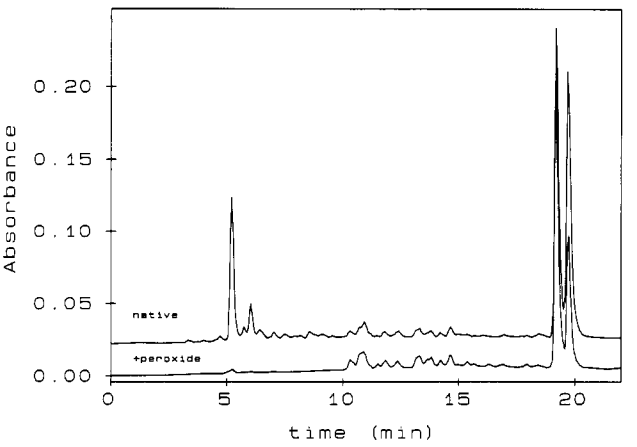

FIGURE 1: Reverse-phase HPLC chromatograms of the pronase digestion of the tryptic peptide containing the P460 heme. The tryptic peptide T7 was isolated from digests of native HAO and then further digested with pronase as described in Materials and Methods to give the top chromatogram. Native HAO was treated with hydrogen peroxide, and then the digestions and chromatography were repeated, to give the bottom trace. The comparison shown is after the second pronase digestion, but as discussed in the text, the tryptic peptides before pronase digestion also had different chromatographic behaviors.

Hydrogen peroxide has previously been shown to react with HAO, resulting in an inactive enzyme (Hooper & Terry, 1977). The effect is localized solely to the P460 heme such that the 463-nm absorption band is no longer present in the dithionite-reduced, H_2O_2-inactivated enzyme. The *c* hemes exhibit no changes in either their optical or redox properties (Collins et al., 1993). The effect of peroxide on the chromatographic properties of the heme-containing peptides was therefore investigated. Both native and H_2O_2-inactivated HAO were digested with trypsin, and the heme peptides were purified through the HPLC gel filtration column. The peaks corresponding to the heme peptides showed no changes in either position or breadth, except for T7. The T7 peak of H_2O_2-inactivated HAO was substantially broadened compared to the T7 peak from the native enzyme. When T7 from H_2O_2-inactivated HAO was further fractionated by reverse-phase HPLC, it eluted as a broader band with noticeable shoulders compared to the peptide from the native enzyme. Since Arciero and Hooper (1993) have shown that T7 contains two hemes that could be separated by further digestion of T7 with pronase, peptide T7 from H_2O_2-inactivated HAO was similarly treated. Figure 1 displays a comparison of a reverse-phase HPLC separation of the pronase peptides derived from native HAO and H_2O_2-inactivated HAO, monitored at the absorbance of the Soret band. It is clear that peroxide treatment resulted in the disappearance of heme peptides eluting near 5–7 m, but had no effect on the heme peptides around 19–20 m. These are the regions of the chromatogram where the Pr1 and Pr2 heme peptides elute, respectively. Thus, while T7 from H_2O_2-inactivated HAO exhibited extensive heterogeneity, the heterogeneity was localized solely to the Pr1 region of the parent peptide. In this particular trial there was one dominant peak in the 5–7-m cluster, and there were two significant peaks around 19–20 m. In other pronase digestions discussed later, as many as three major peaks were observed in the first cluster and the relative sizes of the two peaks around 19–20 m fluctuated. Pronase is a nonspecific protease, and proteolytic heterogeneity, which is a common problem, could account for such changes.

Sequence Analysis. In an earlier report (Arciero & Hooper, 1993), heme peptides T7, T7C, and Pr1 were reported to be cross-linked, yielding two PTH–amino acid derivatives during each cycle of the Edman degradation. Heme peptide Pr2 was not cross-linked, yielding only a single PTH–amino acid derivative during each cycle of the Edman degradation. The data from these sequencing runs as well as data from bromelain- and pepsin-generated heme peptides allowed the following sequences for the two peptide chains in T7 to be assigned.

G-X-T-M-X-H-T-N-Q-N-K-X-D-N-X-H-T-R-H-E-F (chain a)

L-A-H-V-N-P-G-G-W-T-X′-T-E-G-W-G-P-M-N (chain b)

X represents a blank during the Edman cycle but is assumed to represent a Cys residue since the sequence "C-residue-residue-C-H" is the expected pattern for thioether linkages to heme *c*. Amino acid compositions were consistent with the presence of Cys but did not determine the number of such residues. The residue X′ was ambiguous. It could have been Asn on the basis of the detection of a small amount of that PTH derivative at the corresponding cycle during one of the sequencing runs. However, as will be shown later, this residue is involved in the cross-linkage and would generate a blank for the Edman reaction.

Heme Reactivity in the Peptide. Attempts were made to break the covalent bonds between heme and T7C. They included heavy metal methods (Paul, 1950, 1951; Barrett & Kamen, 1961) and the sulfenyl halide method (Fontana et al., 1973) for scission of thioether bonds, and the reduction–alkylation method (Nichol et al., 1987) for breaking disulfide covalent bonds between heme and peptide, such as that found in lactoperoxidase. These methods failed to yield any extractable heme pigment from T7C. Thioether scission by silver sulfate can usually be followed by monitoring the visible spectral change of a heme *c* chromophore from low-spin ferric to high-spin ferric features (Timkovich, 1980). Oxidized T7C had a typical low-spin ferric spectrum, and it did not change during silver sulfate treatment. It will subsequently be shown that T7C does bind hemes by thioether bonds. Breaking one set associated with one heme would not liberate that heme, for reasons that will be explained later, but the second heme should be liberated. The observation was that neither was liberated, nor was the usual spectroscopic change detected. We interpret this result as meaning that the thioether bonds are somehow protected from attack in the peptide.

The pyridine hemochromogen spectrum (Arciero & Hooper, 1993) of T7C demonstrated the usual bands of a *c*-type heme with an α_{max} at 550 nm and a β_{max} at 523 nm. Bands were also slightly broader than for a typical heme *c* pyridine hemochromogen, but this was a very subtle spectral feature. Pyridine hemochromogen spectra for the peptides derived by pronase digestion of T7 or T7C provided major evidence that P460 constitutes a novel structure. The spectrum of Pr2 was indistinguishable from that of heme *c*. The spectra of Pr1a, Pr1b, and Pr1c were clearly different, with broad maxima at 526 and 556 nm. A typical pyridine hemochromogen spectrum for a Pr1 peptide has been reported in Figure 8 of Arciero and Hooper (1993). The most striking feature is the decrease in apparent intensity for the α band (556 nm) relative to the β band (526 nm). The α and β bands of metalloporphyrins (Gouterman, 1978) consist of degenerate transitions due to the pseudo-4-fold symmetry of the mixed π-electron orbitals. A decrease and a broadening of these bands is consistent with a major perturbation in this pseudosymmetry.

Mass Spectrometry Results. LSIMS spectra provided major structural evidence for T7 and peptides derived from it. It has been previously shown (Carraway et al., 1993) that normal heme *c*-containing peptides undergo a characteristic fragmentation in the LSIMS matrix in which the thioether bonds are efficiently cleaved, and the heme rearranges to protonated iron protoporphyrin IX (**1**). This gives an intense

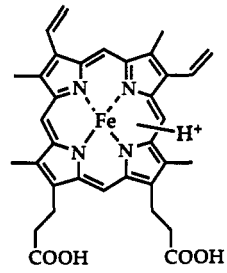

1

ion signal in MS spectra at m/z 617. Positive ion LSIMS spectra of Pr2 showed intense ions at m/z 1308 and 617. The LSIMS matrix normally produces $(M + H)^+$ parent ions, but sodium, potassium, or ammonium adducts can also occur. It is possible to check for the higher mass adducts by negative ion LSIMS, which typically gives the most intense ion signal for $(M - 1)^-$. For Pr2, negative LSIMS produced ions with m/z 1306 and 690, thereby proving that the positive ion 1308 was indeed the proton adduct. The negative ion 690 corresponds to the peptide backbone *without* covalently attached heme but with the two Cys residues. The cleaved, free heme did not give an observable negative ion signal, consistent with earlier reports based on other heme peptides (Carraway et al., 1992). Linked-scan experiments (Jennings & Mason, 1983) were also performed to prove that the 617 ion was indeed a daughter fragment of the 1308 parent and not an ion arising from a noncovalent impurity. Amino acid sequencing and composition analysis indicated that the peptide in Pr2 had the sequence X-Asp-Asn-X-His-Thr, where X was a blank on that Edman cycle, as discussed previously. Cys was detected in compositions. High-resolution LSIMS determined that the 617 ion had an exact mass of 617.183, and since the calculated mass of protonated iron protoporphyrin IX is 617.185, this confirmed the heme in Pr2 as arising from normal heme *c*. These results were the first evidence beyond visible spectroscopy that a "normal" heme in HAO was an authentic cysteine-substituted iron protoporphyrin IX. Although the heme was unlikely to be otherwise, visible spectroscopy has limitations, and the identification is now on firmer ground. The exact mass of the $(M + H)^+$ ion (1308.400) corresponded to the above peptide sequence with X equal to Cys (calcd 1308.391). The parent T7 thus contains 1 equiv of authentic heme *c*, and one covalent attachment site for it, plus something else.

In order to understand the MS analysis for the most purified Pr1 peptides, it will be helpful to first discuss results obtained on an unfractionated mixture of peptides derived from an extended pronase digestion of T7C. Extended pronase digestion produced the smallest peptide fragments, but it also produced the most heterogenous mixtures, because of the broad specificity of pronase. Yields of single, purified products were too low for practical large-scale preparation of material for sequence or NMR studies. However, MS results can be obtained from mixtures even if the compounds are present at low levels. LSIMS analysis of unfractionated, extended pronase digests of T7C afforded some important facts that

relate to the P460 structure. Below m/z 500, the spectrum showed a complicated mixture of many ions, consistent with diverse small peptides. At high mass there were five observable ions at m/z 1548.5, 1447.5, 1308, 796, and 617. Linked scans demonstrated that 617 was a daughter ion from the 1308 parent, thus establishing that these two ions were from Pr2 that was present in the mixture. Linked scans also demonstrated that 617 was not a fragment from either 1548 or 1447, but that 796 was a fragment from both of these. Linked scans from the 617 and 796 ions showed that they further fragmented in very similar ways, including loss of 14 (minus CH_3, plus H), 45 (minus CO_2H), 59 (minus CH_2CO_2H), and 73 mass units (minus $CH_2CH_2CO_2H$). In high-resolution spectra, the observed exact mass of the 796 ion was 796.245. The calculated exact mass of protonated iron protoporphyrin IX plus the amino acid tyrosine and minus two hydrogens is 796.243. The data indicated that, in addition to heme *c*, there was a *second* heme present that was like heme *c* but had an additional covalent attachment to a tyrosine residue. This new bond replaced one X–H bond on the tyrosine and one on the heme.

One relatively large scale but short duration pronase digestion of T7 gave a major Pr1 peptide, which was subjected to sequence analysis. The results of seven Edman cycles were as follows:

cycle	1	2	3	4	5	6	7
PTH derivative	G	T	T + E	G + M	blank	H	T

An additional pronase digestion was performed to produce more material for MS and NMR analysis. In this preparation, in addition to the major fraction, designated Pr1a, two more fractions, designated Pr1b and Pr1c, were resolved by reverse-phase HPLC in the Pr1 window illustrated in Figure 1.

Positive ion LSIMS spectra of the purified peptides showed major ion peaks at m/z 1835.7 and 1083 for Pr1a and 1936.6 and 1184 for both Pr1b and Pr1c. From this result and the NMR spectra of Pr1b and Pr1c to be discussed, it appeared that fractions 1b and 1c contained the same heme peptide. It is not clear why they were partially resolved during HPLC, but it could have been due to conformational isomerism, such as different fifth or sixth heme ligand bonds. Negative ion LSIMS demonstrated that the high-mass ions were in each case indeed the $(M + H)^+$ ions, and linked scans proved that the lighter ion in each case was a daughter fragment from the heavier parent. Literature precedents and the prior work on the T7C mixture indicated that the daughter ions were fragments produced by cleavage of thioether bonds and rearrangement of the heme to protonated iron protoporphyrin IX. The masses were consistent with the partial sequence of T7 and allowed the assignment of the ions as indicated in Table I. The MS data are strongly in accord with P460 being a heme *c* with an additional covalent cross-link to another peptide segment via the side chain of tyrosine. The MS data for Pr1a are in accord with the prior sequence data when one realizes that there are *two* peptides present and *three* covalent bonds to heme. The PTH derivatives released by the Edman reaction were as follows:

cycle	1	2	3	4	5	6	7
chain a	G	blank (Cys)	T	M	blank (Cys)	H	T
chain b	blank (Y)	T	E	G			

NMR Results. NMR spectroscopy on heme peptides has been attempted only infrequently. The spectrum of highly purified heme peptides prepared from horse heart cyt *c* was obtained after special precautions were taken to prevent oligomerization and force conversion to a low-spin ferric cyano heme complex (Kimura et al., 1981). It would be unfeasible to assign structure *de novo* using such spectra because the iron paramagnetism causes *a priori* unpredictable chemical shifts and line broadening. NMR spectra of T7C in the ferric state were examined, but they could not be structurally interpreted. T7C showed extensive contact- or pseudocontact-shifted bands between −10 and 32 ppm, with line widths and shifts consistent with a low-spin ferric electronic state (*vide ante* the optical spectrum). The discrete signals suggested at least a partially ordered, as opposed to a random, structure. The order could account for the earlier observation that thioether bonds in T7 were resistant to attack by common reagents. We have also investigated heme peptides from horse cyt *c* in a diamagnetic state as the ferrous CO complex. Because of the well-known *trans* effect for metal carbonyl binding (Atwood, 1985), it is expected that the ferrous iron would be complexed to one CO and the histidine side chain. Ferrous, CO-complexed heme peptides from horse cyt *c* showed narrow resonances confined to the usual diamagnetic range, but they also showed extensive conformational heterogeneity, manifested by chemical exchange broadening and even the disappearance of expected resonances. The ferrous CO complex of T7C demonstrated similar problems of conformational heterogeneity. The optical spectrum was typical of low-spin (i.e., diamagnetic) ferrous *c*-type cytochromes with a 550-nm α band. Its ^{1}H-NMR spectrum over a wide temperature range showed only broad, featureless lumps in the aliphatic and aromatic regions and no paramagnetically shifted resonances. NMR samples were treated with pronase in an attempt to cleave off residues and produce a smaller heme peptide less susceptible to conformational heterogeneity. There were encouraging results in that even though the mixture was complex, sharp well-defined resonances began to appear, especially in the meso region around 10 ppm where no amino acid resonances are expected. This indicated that the spectra of purified pronase peptides from T7 might yield useful structural information.

^{1}H-NMR spectra of purified pronase peptides were initially confusing until temperature studies were performed. Figure 2 contrasts the ^{1}H-NMR spectra of Pr1c in the expected meso proton region at different temperatures. For a single heme bonded to the peptide, four singlets are expected. At low temperature multiple peaks were seen, but note the tendency to three clusters. Peaks coalesced as the temperature was raised, reaching a minimum line width around 333 K, but then broadened again as the temperature approached the boiling point. This behavior can be interpreted in terms of conformational heterogeneity. At low temperatures some

Table I: Mass Spectral Data Interpretation for P460-Containing Peptides

PR1b	PR1a	peptides in exhaustive pronase digest of T7C	
m/z 1936.7	m/z 1835.7	m/z 1548.5	m/z 1447.4
G-C-T-M-C-H-T heme c T-Y-T-E-G	G-C-T-M-C-H-T heme c Y-T-E-G	G-C-T-M-C-H-T heme c Y	G-C-T-M-C-H heme c Y

Corresponding Daughter Fragments from Thioether Cleavage

m/z 1184	m/z 1083	m/z 796	m/z 796
FePPIX+H+ T-Y-T-E-G	FePPIX+H+ Y-T-E-G	FePPIX+H+ Y	FePPIX+H+ Y

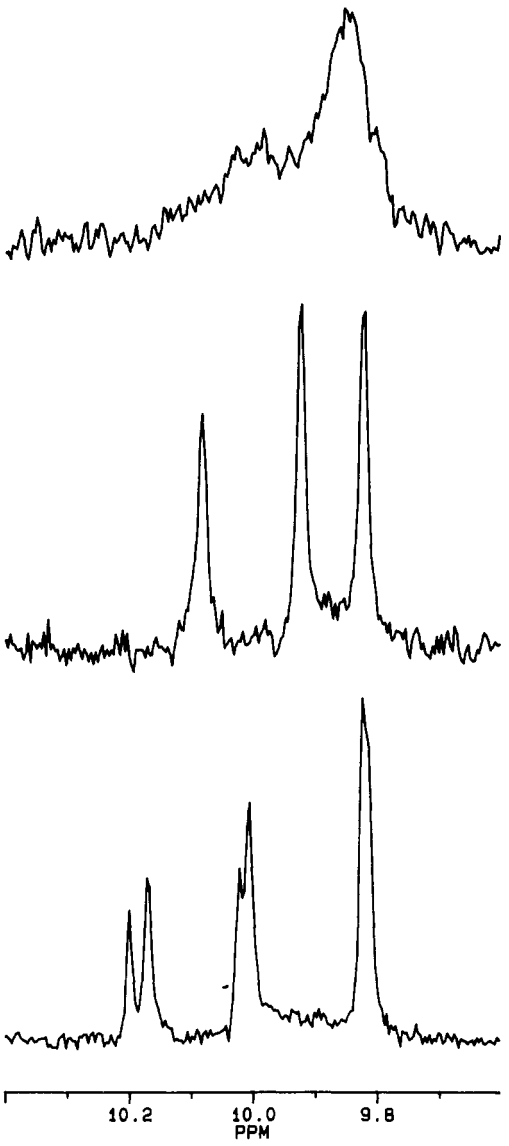

FIGURE 2: The meso region of the ^{1}H-NMR spectrum of the P460 heme peptide Pr1c. The lower trace is at 298 K; the middle, at 333 K; and the top, at 360 K.

conformations are in very slow exchange leading to resolved resonances representing the different environments. As the temperature is raised, the rate of exchange increases and lines coalesce to the time average. But it appears there are additional conformations that become accessible at higher temperatures, and exchange among these newly accessible states then causes line broadening again.

All Pr heme peptides behaved the same way with all resonances affected, albeit to different extents. The peptides contained impurity peaks due to contaminating peptides. The contaminants were different for Pr1a, -b, and -c, but it was readily possible to identify the resonances that belonged uniquely to Pr heme peptides because of their consistency. The temperature behavior was reversible. Ferrous CO-complexed samples were highly stable and showed no spectral changes over months of time.

Coupled spin systems were determined for the Pr peptides by two-dimensional HOHAHA spectroscopy (Bax & Davis, 1985a; also known as TOCSY) in ^{2}H2O or ^{1}H2O (Driscoll et al., 1989). In principle, NH resonances could also be observed and assigned in such spectra in ^1H_2O, but the Pr peptides gave very poor spectra in protic water. We were limited in quantities by the yield and solubility of the peptides, and the dynamic range problem of working in a protic solvent was very severe. Also, the amide resonances were extremely broad and difficult to detect even in simple one-dimensional spectra taken with presaturation of the water or with selective excitation pulse sequences (Plateau & Gueron, 1982; Clore et al., 1983). It is possible that solvent exchange in such small peptides on top of the other conformational heterogeneity just makes observation impossible. The NMR spectra of Pr1b and -1c were the same for resonances assigned to the Pr peptide, although they did have different impurities.

Two-dimensional HOHAHA spectra in ^{2}H2O provided important evidence for the assignment and identification of the peptide and heme resonances. This experiment shows all spin-coupled resonances in isolated spin subsystems. A portion of the two-dimensional HOHAHA spectra of Pr1a is shown in Figure 3.

Amino acid resonances due to the peptides were assigned by characteristic coupling patterns and chemical shifts to residue spin subsystems. Because of the small number of residues, some specific assignments were accomplished, even though sequential assignment in the conventional sense was not possible because of the poor spectra in protic water. The assignments are summarized in Table II. The glycine subsystems were readily assigned because of the unique nature of two coupled α protons. The abnormally low frequency shifts assigned to Gly 1 are believed to be due to a ring current shift by the heme plane. The spin systems of Cys, His, and Tyr are of the AMN type. The resonances of His 6 were assigned on the basis of analogy to the heme ligand histidine observed in cytochromes *c*-551 from *Pseudomonas aeruginosa* and *Pseudomonas stutzeri* (Chau et al., 1990; Cai et al., 1992). In any *c*-type heme, the span from the first thioether bridge cysteine residue to the histidine ligand is short, and there are only limited conformational possibilities for the peptide segment because of three bonds anchoring it to the heme. Therefore, there should be good analogy between the present heme peptides and full *c*-type cytochromes in this region. The α and β protons of His 6 are at low chemical shifts because the residue is a heme ligand and the protons experience a strong, low-frequency ring current shift. There were two AMN spin subsystems in the P460 peptides that closely matched the chemical shifts found in cyt *c*-551's (one cysteine close to 5 ppm, the other close to 4 ppm), and so by analogy these were assigned to Cys 2 and Cys 5, respectively. The remaining AMN subsystem was assigned to Tyr 2′ by a process of elimination. If one did not rely upon the analogy to cyt *c*-551, then these AMN sets would not be assignable to specific sites, but the observed resonances would still be fully consistent with the Edman sequencing and mass spectral results. Methionine and glutamic acid both have similar spin subsystem coupling patterns, but the chemical shifts of the γ protons are characteristically different. This allowed simple assignment in the P460 peptides, where the observed values closely matched expected shifts for these residues in common peptides and proteins (Grob & Kalbitzer, 1988). Threonine has a unique ABX_3 spin subsystem, and these residues were readily evident in the observed spectra. Thr 3′ was simple to assign because it appeared in the spectrum of Pr1b but not Pr1a. The resonances assigned to Thr 3′ were present in both Pr1b and Pr1a but experienced about a 0.1 ppm shift, while the remaining two subsystems were very constant in both peptides. Since these peptides differ in sequence by the addition of Thr 1′ to Pr1b, it was reasonable to assign the most perturbed set to Thr 3′. No evidence was available to distinguish the Thr 3 and Thr 7 resonances.

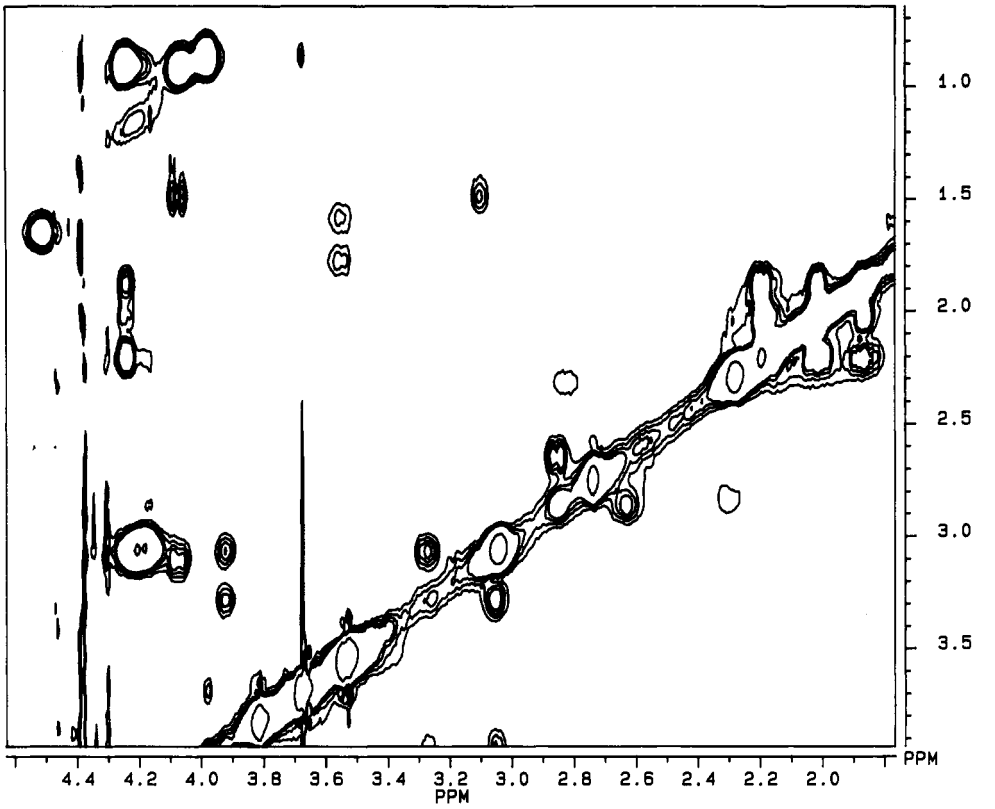

FIGURE 3: Portion of the two-dimensional HOHAHA spectrum of the P460 heme peptide Pr1a at 333 K. The sample concentration was approximately 0.25 mM. The spin-lock time was 44 ms, and the digital resolution was 3.3 Hz in F_2 and 26.4 Hz in F_1, zero-filled to 6.6 Hz before Fourier transformation. The ridges at 4.4 ppm parallel to the vertical axis are due to the residual HDO peak, and the ridge at circa 3.7 ppm is due to a trace of tris(hydroxymethyl)aminomethane buffer. Critical features from this region are as follows. The cross peak at 4.5 and 1.6 ppm is due to the low frequency shifted thioether bridge methine–methyl. The heme methyl singlets are observable on the diagonal at 3.8 and 3.5 ppm (two partially resolved resonances), and the low frequency shifted methyl is observable at 2.77 ppm. The intense cross peak at 4.2 and 3 ppm is due to the heme propionate methylenes. Other assigned resonances are listed in Table II.

The remaining resonances provided critical information to identify the heme in the P460 peptides as normal heme *c*, but with an additional point of covalent attachment to peptide. One heme thioether methine and methyl subsystem, three heme methyls, and two heme propionate subsystems showed normal chemical shifts that were very close to their counterparts in cyt *c*-551. Unique features included only *three* meso proton resonances and heme methyl and thioether methine–methyl subsystems, both shifted to abnormally low frequencies. The aromatic region from 7 to 8 ppm was initially confusing because of multiple peaks. As discussed previously, the Edman sequencing data was ambiguous and showed a blank on the cycle that should have liberated the 2′ residue; the MS data conclusively indicated for this position a mass corresponding to a tyrosine residue missing one proton, but MS could not establish which proton. By examination of multiple samples from different preparations, it became evident that there were always three broad resonances of area one proton each in the 7–8 ppm region, intermixed with sharp resonances due to aromatic protons from contaminating non-heme peptides. The impurities could be so identified because they had variable areas in different samples, and the peptides Pr1a, -1b, and -1c had different sets of impurity peaks. In spite of rechromatography efforts, we have not been able to eliminate these contaminants, but we are confident that they are contaminants because of their variability. HOHAHA spectra indicated that two of the three broad aromatic resonances were spin-coupled to each other but not to anything else, and the remaining resonance was indeed a singlet.

The key to interpreting the perturbed heme resonances was provided by a previous precedent in the literature (Yap-Bondoc & Timkovich, 1990). Phenylhydrazine is a suicide inhibitor of the bacterial nitrite reductase termed cytochrome cd_1. When phenylhydrazine is used as a reductant for the enzyme, a radical-based reaction occurs that creates a phenyl radical. This in turn regiospecifically attacks the heme d_1 prosthetic group and replaces the proton at the 5-*meso* position. Isolation and purification of the metal-free derivative porphyrin d_1 afforded an NMR spectrum with only three meso resonances. The aromatic protons from the attached phenyl group appeared as five discrete resonances. Molecular modeling calculations indicated that there was a high barrier to rotation for a meso phenyl group and the porphyrin contained two chiral centers, one directly adjacent to the 5-*meso* position. The situation is highly similar to the P460 peptides, that is, only three meso protons and three aromatic tyrosine protons. On the basis of only the mass data, the tyrosine ring could have been bonded through the oxygen, but then four aromatic protons, as two spin-coupled pairs, should have been present in the NMR spectrum. The hydroxyl proton of tyrosine is exchangeable and so was not observable in any NMR experiment.

The similarity between these cases is even stronger. The phenyl protons in phenyl-substituted porphyrin d_1 were at normal chemical shifts. The phenyl ring was constrained to be perpendicular to the porphyrin plane, and in this orientation there is negligible ring current perturbation on the phenyl protons. However, the phenyl ring caused a 1.6 ppm shift to lower frequency for an acetate proton that was adjacent to the meso site and a 0.3 ppm shift for an adjacent porphyrin ring methyl. In the P460 peptides, one perturbed thioether methine proton has shifted to lower frequency by 1.9 ppm, and one heme methyl has shifted by circa 0.7 ppm. The shifts of a

Table II: ^{1}H-NMR Assignments and Chemical Shifts for the P460 Heme Peptides

assignment	chemical shift Pr1a	Pr1b
meso's	10.07, 9.90	10.08, 9.93
15-*meso*	9.82[a]	9.83
thioether methine	6.39	6.41
thioether methyl	2.28	2.31
thioether methine	4.51	4.52
thioether methyl	1.63	1.64
heme 13^1,17^1 methylene	4.20, 4.18	4.24, 4.19
heme 13^2,17^2 methylene	3.07d[b]	3.07, 3.05
heme methyls	3.80, 3.54, 3.52	3.83, 3.58, 3.55
	2.77	2.76
Gly 1 α	2.83, 2.32	2.84, 2.35
Cys 2 α[c]	4.89	4.95
Cys 2 β	2.86, 2.63	2.87, 2.62
Met 4 α	4.25	4.30
Met 4 β	2.20, 1.86	2.23, 1.90
Met 4 γ	2.01d	2.04d
S-CH3	2.29	2.32
Cys 5 α	3.95	3.93
Cys 5 β	3.27, 3.06	3.30, 3.06
His 6 α	3.54	3.57
His 6 β	1.77, 1.59	1.78, 1.59
Thr 1'α[d]		3.10
Thr 1'β		3.74
Thr 1'γ		0.87
Tyr 2'α[e]	4.72	4.84
Tyr 2'β	3.40, 3.12	3.43, 3.12
ring H	7.73so[f]	7.75sc
	7.54sc	7.55sc
	7.42	7.42
Thr 3'α[g]	4.25	ND[h]
Thr 3'β	4.06	4.14
Thr 3'γ	0.92	1.05
Glu 4'α	4.08	4.11
Glu 4'β	1.49, 1.32	1.49, 1.35
Glu 4'γ	3.06d	3.10d
Gly 5'α	4.20, 2.82	4.18, 2.83
Thr 3,7 α	3.70[i]	3.72
Thr 3,7 β	4.27, 3.98	4.27, 3.99
Thr 3,7 γ	0.90, 0.86	0.91, 0.88

[a] Assigned by rotating-frame enhancement from this chemical shift to the shift of the propionate methylenes. [b] The symbol "d" indicates that two protons are accidently degenerate. [c] Assigned by analogy to cyt *c*-551 as discussed in the text. [d] Assigned because it was present in Pr1b but not in Pr1a. [e] Assigned to Tyr 2' as the only unaccounted for spin system with high-frequency β protons. The assignments of Cys 5 and Tyr 1' could be interchanged, although the present assignment is considered more likely on the basis of analogy to cyt *c*-551. [f] These are spin-coupled to each other. [g] Although this resonance was present in both Pr1a and Pr1b, of the three Thr spin systems in Pr1a, this one experienced the largest shift change in Pr1b, as might be expected for addition of Thr 1' to Pr1b. [h] Not determined. Believed to have shifted under the residual water peak, which obscures a retangular region in the two-dimensional spectrum from 4.25 to 4.5 ppm. [i] The 3.70 ppm α proton belongs to the 3.98, 0.86 ppm spin system. The α proton for the other system is probably buried under the residual water peak.

thioether methine and a methyl thereby establish that the tyrosyl ring must be bonded to either the 5- or 10-position but do not say which one.

The P460 peptide pyridine hemochromogen optical spectrum was unusual in terms of the wavelength shifts, the band broadness, and the low intensity of the α band relative to the β and Soret bands. Tyrosyl addition at a meso position qualitatively could account for the effects. Normal free-base porphyrins have a 5-band optical spectrum. In diamagnetic metalloporphyrins such as low-spin ferrous heme (the pyridine hemochromogen electronic state), the core becomes pseudo-4-fold and electronic transitions become degenerate, leading to a 3-band (α, β, and Soret) spectrum. Tyrosyl addition at a meso position could be enough of a perturbation that even the pseudo-4-fold symmetry is disrupted. The band broadening could be the result of partial separation of the transition degeneracy, and the apparent loss of intensity is actually just a redistribution across the broad band. A previous resonance Raman study (Andersson et al., 1991) was not able to fully identify the structure of the P460 heme but indicated it had novel characteristics with symmetry properties lower than that of protoporphyrin IX.

Conformational and Isomer Analysis. Two structure issues remain. What meso site and what tyrosyl ring position are involved in the covalent attachment? The NMR and MS data have narrowed this down to four possibilities: Tyr C2 to 5-*meso*, Tyr C2 to 10-*meso*, Tyr C3 to 5-*meso*, or Tyr C3 to 10-*meso*. Because the peptide bridge between the two normal thioether bonds spans the 5-*meso* site, an initial question was whether the 5-position could even be possible without steric hindrance. Molecular modeling calculations were performed using XPLOR (Kuszewski et al., 1992) to investigate conformational possibilities. Although the combinations involving Tyr C2 or 5-*meso* lead to more compact structures, none of the four isomers could be ruled out on energetic grounds. All combinations could be accommodated by rotations about free bonds without van der Waals or energy violations and with comparable final energies after refinement.

In principle the isomer question could be solved by measuring appropriate nuclear Overhauser effects between neighbor protons. The size of the P460 peptides places these molecules at a correlation time where the sign of the NOE is changing from positive to negative, and hence longitudinal effects are near 0 at 500 MHz. At lower field strengths there is insufficient sensitivity for practical results. An approach to the problem is the use of rotating frame nuclear Overhauser measurements such as CAMELSPIN (Bothner-By et al., 1984) or its two-dimensional version, ROESY (Bax & Davis, 1985b). However, rapid relaxation and short T_1, T_2, and $T_{1\rho}$ times may still lead to very rapid decay of coherences, in which nonspecific relaxation may dominate the specific relaxation which gives rise to the Overhauser enhancement. Normal one- and two-dimensional NOE experiments and the rotating-frame experiments ROESY and CAMELSPIN were attempted at 360 and 500 MHz for the P460 peptides. Only a few, very weak enhancements were seen. There was a weak enhancement from the lowest frequency meso proton to the propionate methylene resonances, which allowed assignment of this meso as position 15. Consider Figure 4. If the tyrosyl ring were at the 10-*meso* position, then the perturbed heme methyl would be at the 12-position and it would be expected to give an enhancement to the propionate resonances at position 13. If the tyrosyl ring were at the 5-*meso* position, then the perturbed methyl would be at position 7 and the expected enhancement would be to the normal thioether at position 8. In the lowest energy calculated conformation for the isomer substituted at the 5-*meso* position, the closest neighbor to the 7-methyl substituent is the 8-position thioether methyl with a carbon–carbon distance of 3.3 Å. There was a weak NOE from the perturbed heme methyl at 2.77 ppm in Pr1a to the normal thioether methyl at 2.28 ppm, as shown in Figure 5. This suggests that the substitution was at position 5. Unfortunately, this was the sole piece of evidence relating to isomer assignment, and in the absence of further confirmations, the assignment should be considered tentative.

No nuclear Overhauser enhancement information was observed to indicate which tyrosyl ring position was involved in the bond. C3 and C5 are ortho to the tyrosine hydroxyl and are expected by simple resonance stabilization arguments

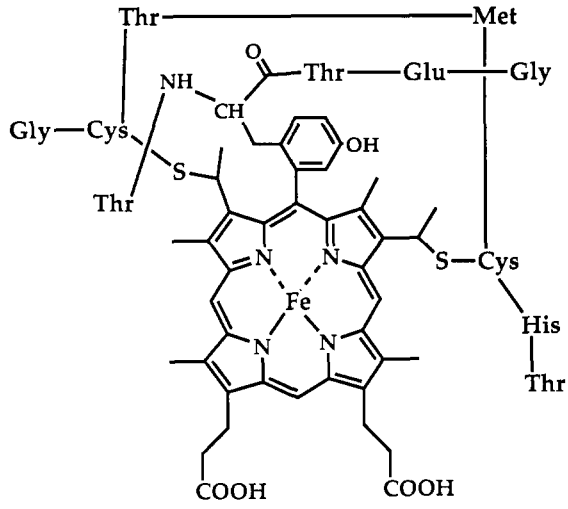

FIGURE 4: Schematic diagram showing the heme plane of P460 cross-linked to two peptides via the cysteine thioether linkages and the tyrosyl–heme linkage.

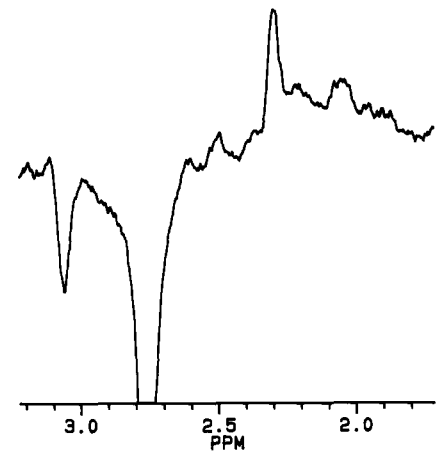

FIGURE 5: Difference spectrum (reference minus cross-relaxation) showing the rotating-frame nuclear Overhauser effect (ROE) obtained upon irradiation of the perturbed methyl at 2.77 ppm in the ferrous CO-complex of the P460 peptide Pr1a. The CAMELSPIN sequence (Bothner-By et al., 1984) was employed with a 75-ms spin-locking field of 4 W and a semiselective inversion pulse applied at 2.77 ppm in the cross-relaxation spectrum. ROEs are antiphase with respect to the irradiated resonance, and the weak enhancement to the normal thioether methyl appears as the positive peak at 2.25 ppm. The 2.77 ppm resonance is broad and requires relatively high power, short duration pulses for inversion, so that the irradiating frequency is not perfectly selective. The negative feature at 3.0–3.1 ppm is due to excitation of a neighboring strong peak due to overlapping resonances from heme methylene propionates and Cys 5 CβH, Tyr 2′ CβH, and Glu 4′ CγH protons.

to be the most reactive sites for a radical-based substitution reaction. However, an alternative tentative assignment to C2/C6 is favored on the basis of the observed chemical shifts and an argument relying upon shift analogy. In simple peptides, the two highest frequency resonances are typically C2 and C6, with C3 and C5 at lower frequency, although the gap is not large between the two sets. In the P460 peptides, the tyrosyl protons are two relatively low frequency resonances, one of which is spin-coupled to the highest frequency resonance, while a second high-frequency peak is absent. The argument is marginal, but it does suggest that C2 or C6 (which are indistinguishable in this case) is the point of attachment to the heme.

DISCUSSION

How does the tyrosyl ring become attached to heme *c* to form the P460 heme peptide? There are no biosynthetic precedents for a reaction pathway to form the novel carbon–carbon bond, and we think it is highly unlikely that it is formed by the action of an independent biosynthetic pathway. It seems more likely that the enzyme first exists in a form that can be designated "pre-P460" in which it contains normal heme *c* and a normal tyrosine side chain in the future P460 heme crevice. At some point the linkage is formed *in situ* as a result of reactions that take place in this heme crevice to generate the final form of HAO. Precedent for radical production and heme attack may be found in the covalent addition of a phenyl ring to the heme d_1 of cyt cd_1 after a phenyl radical is created by mistake during oxidation of phenylhydrazine linked to reduction of heme d_1. The phenyl-d_1 investigation followed a very large body of work by Ortiz de Montellano and co-workers on the formation of regiospecifically modified hemes in hemoproteins. Of the many cases studied by this group, the most relevant to us was their investigation of a heme–protein cross-link in peroxide-treated myoglobin (Catalano et al., 1989). They obtained very firm mass spectral, chromatographic, and amino acid composition evidence that upon H_2O_2 treatment up to 18% of the myoglobin sample formed a new covalent bond to Tyr 103 of the protein. They did not identify the actual covalent bond by direct evidence, but on the basis of other considerations, they suggested that the most likely bonding arrangement was between an ortho tyrosyl ring carbon and a meso of the heme, perhaps meso 20 since it is closest to Tyr 103 in the myoglobin crystal structure. A mechanism of formation was proposed involving a tyrosyl radical generated during formation of the iron ferryl state by peroxide.

An important issue is when the conversion from pre-P460 to P460 occurs. We have considered whether there may be a stable tyrosyl radical at the active site in the native resting state of the enzyme that forms the covalent bond during denaturation of the enzyme in preparation for enzymatic digestion. It is impossible to unequivocally rule this out, but there are some considerations that render it unlikely. The radical would have to be in an unusual environment to be stabilized in the native resting state of the enzyme. It is not clear how such a radical could lead to the unique spectroscopic features of P460 in the holoenzyme, since then the heme would be normal heme *c*. If the radical exists, why would its reactions during denaturation be so regiospecific as to lead to a single covalent bond on the heme? At the present time there is no evidence that the P460 heme site is heterogeneous in the holoenzyme. The P460 heme is marked by its unique spectroscopic properties in the native isolated enzyme, and these are constant over many preparations. Enzymatic digestion and chromatography does lead to less than 100% recovery of the P460 heme peptide, and there is heterogeneity in the digestions such as that illustrated by the minor peaks in Figure 1. However, this is to be expected for enzymatic hydrolysis of a complicated protein using pronase. The P460 heme peptides discussed in this and the previous article (Arciero & Hooper, 1993) have consistently been the main components isolated in many different preparations.

At the other logical extreme, one could envision that pre-P460 is not yet the mature form of HAO. In this state, the protein has a tendency to promote radical chemistry that leads to a tyrosyl radical or a porphyrin-based radical that initiates formation of the resulting novel P460 center. As mature P460, the site is then resistant to or incapable of further radical reactions that do not involve its main catalytic functional cycle. Viewed in this light, the formation of the P460 heme is just

another example of a pre-enzyme or zymogen undergoing activation. In this case, there is self-activation, or the autobiosynthesis of the P460 heme, in the sense that no other external enzyme activity is responsible for bond formation.

What possibilities exist for radical-based chemistry at the active site of pre-P460? HAO converts hydroxylamine plus water into nitrite, protons, and electrons that are transferred ultimately to an acceptor cytochrome *c*-554.

$$NH_2OH + H_2O \rightarrow NO_2^- + 4e^- + 5H^+$$

During the catalytic cycle, electrons are removed from hydroxylamine (an oxidation) and transferred to the multiple *c* hemes of HAO (reduction), which are then reoxidized by the acceptor *c*-554. Generation of a neutral tyrosyl radical in the active site of pre-P460 would be a formal oxidation (removal of a proton and an electron). The standard reduction potentials for mature HAO have been measured (Collins et al., 1993), and the *c*-type heme potentials range from −412 to 288 mV versus the normal hydrogen electrode. The P460 heme potential is at −260 mV at pH 7.0. No site in the mature enzyme is therefore a strong enough oxidizing agent by itself to account for facile electron abstraction from a tyrosine. However, in pre-P460, the potentials would not have to be the same, especially at the future P460 site. Perhaps pre-P460 is activated by hydrogen peroxide to generate the radical, as described for myoglobin (Catalano et al., 1989). Another possibility could be activation by O_2, in which the pre-P460 site, with or without electron-transfer reactions to other hemes, is converted into a ferryl or perferryl reactive state. It is difficult to be more precise in these hypotheses at this time. As strange as they may seem, we feel they are preferable to postulating a totally unprecedented biosynthetic transformation.

REFERENCES

Andersson, K. K., Kent, T. A., Lipscomb, J. D., Hooper, A. B., & Munck, E. (1984) *J. Biol. Chem. 259*, 6833–6840.

Andersson, K. K., Babcock, G. T., & Hooper, A. B. (1991) *Biochem. Biophys. Res. Commun. 174*, 358–363.

Arciero, D. M., & Hooper, A. B. (1993) *J. Biol. Chem. 268*, 14645–14654.

Atwood, J. D. (1985) *Inorganic and Organometallic Reaction Mechanism*, p 120, Brooks-Cole Publishing Co., Wadsworth, Inc., Belmont, CA.

Barrett, J., & Kamen, M. D. (1961) *Biochim. Biophys. Acta 50*, 573–575.

Bax, A., & Davis, D. G. (1985a) *J. Magn. Reson. 65*, 355–360.

Bax, A., & Davis, D. G. (1985b) *J. Magn. Reson. 63*, 207–213.

Bothner-By, A. A., Stephens, R. L., Lee, J., Warren, C. D., & Jeanloz, R. W. (1984) *J. Am. Chem. Soc. 106*, 811–813.

Cai, M., Bradford, E. G., & Timkovich, R. (1992) *Biochemistry 31*, 8603–8612.

Carraway, A. D., Burkhalter, R. S., Timkovich, R., & Peterson, J. (1993) *J. Inorg. Biochem.* (in press).

Catalano, C. E., Choe, Y. S., & Ortiz de Montellano, P. R. (1989) *J. Biol. Chem. 264*, 10534–10541.

Chau, M. H., Cai, M., & Timkovich, R. (1990) *Biochemistry 29*, 5076–5087.

Clore, G. M., Kimber, B. J., & Gronenborn, A. M. (1983) *J. Magn. Reson. 54*, 170–173.

Collins, M. J., Arciero, D. M., & Hooper, A. B. (1993) *J. Biol. Chem. 268* (in press).

Driscoll, P. C., Clore, G. M., Beress, L., & Gronenborn, A. M. (1989) *Biochemistry 28*, 2178–2187.

Fontana, A., Veronese, F. M., & Boccu, E. (1973) *FEBS Lett. 32*, 135–138.

Gouterman, M. (1978) in *The Porphyrins* (Dolphin, D., Ed.) Vol. III, pp 1–166, Academic Press, San Diego.

Grob, K. H., & Kalbitzer, H. R. (1988) *J. Magn. Reson. 76*, 87–99.

Hooper, A. B., & Terry, K. R. (1977) *Biochemistry 16*, 455–459.

Hooper, A. B., Maxwell, P. C., & Terry, K. R. (1978) *Biochemistry 17*, 2984–2989.

Hooper, A. B., Tran, J. M., & Balny, C. (1984) *Eur. J. Biochem. 141*, 565–571.

Jennings, K. R., & Mason, R. S. (1983) in *Tandem Mass Spectrometry* (McLafferty, F. W., Ed.) pp 197–222, Wiley-Interscience, New York.

Kimura, K., Peterson, J., Wilson, M. T., Cookson, D. J., & Williams, R. J. P. (1981) *J. Inorg. Biochem. 15*, 11–25.

Kuszewski, J., Nilges, M., & Brunger, A. T. (1992) *J. Biomol. NMR 2*, 33–56.

Lipscomb, J. D., & Hooper, A. B. (1982) *Biochemistry 21*, 3965–3972.

Lipscomb, J. D., Andersson, K. K., Munck, E., Kent, T. A., & Hooper, A. B. (1982) *Biochemistry 21*, 3973–3976.

Nichol, A. W., Angel, L. A., Moon, T., & Clezy, P. S. (1987) *Biochem. J. 247*, 147–150.

Paul, K. G. (1950) *Acta Chem. Scand. 4*, 239–244.

Paul, K. G. (1951) *Acta Chem. Scand. 5*, 389–405.

Plateau, P., & Gueron, M. (1982) *J. Am. Chem. Soc. 104*, 7310–7311.

Prince, R. C., & Hooper, A. B. (1987) *Biochemistry 26*, 970–974.

Prince, R. C., Larroque, C., & Hooper, A. B. (1983) *FEBS Lett. 163*, 25–27.

Timkovich, R. (1980) *Biochem. J. 185*, 47–57.

Yap-Bondoc, F., & Timkovich, R. (1990) *J. Biol. Chem. 265*, 4247–4253.